Research Article | Vol. 24, No. 26 | 26 Dec 2016 | OPTICS EXPRESS 29568
Optics EXPRESS

Field-symmetrization to solve luminance deviation between frames in a low-frequency-driven fringe-field switching liquid crystal cell

MIN SU KIM,[1,3] PHILIP J. BOS,[1] DONG-WOO KIM,[1] CHANG-MIN KEUM,[2] DENG-KE YANG,[1] HYEONG GYUN HAM,[3] KWANG-UN JEONG,[3] JOONG HEE LEE,[3] AND SEUNG HEE LEE[3,*]

[1]*Liquid Crystal Institute, Kent State University, Kent, OH 44242, USA*
[2]*Department of Physics, Kent State University, Kent, OH 44242, USA*
[3]*Applied Materials Institute for BIN Convergence, Department of BIN Convergence Technology and Department of Polymer Nano Science and Technology, Chonbuk National University, Jeonju, Jeonbuk 561-756, South Korea*
[*]*lsh1@chonbuk.ac.kr*

Abstract: The development of low-frequency-driven liquid crystal displays (LCDs) has recently received intense attention to open up low-power consumption display devices, such as portable displays, advertising panels and price tags. In fringe-field switching (FFS) LCD mode, a unidirectional electric field gives rise to head-tail symmetry breaking in liquid crystals, so that the flexoelectric effect, a coupling between the elastic distortion and the electric polarization, becomes enormously significant. The effect is thus linked to an unusual optical effect, which badly damages the quality of images by image-flickering, and this image-flickering is mainly caused by transmittance difference between the applied signal frames. Here, we intensively investigate the mechanism of the transmittance deviation, and propose an essential and promising approach to solve the poor image-quality, that is, symmetrization of electric fields between the frames. The result of our work clearly demonstrates that the field-symmetry is crucial to reduce the image-flickering, and it can be obtained by optimization of the thickness of an insulation layer with respect to the ratio of the space between electrodes to the electrode width.

OCIS codes: (160.3710) Liquid crystals; (230.2090) Electro-optical devices; (230.3720) Liquid-crystal devices.

References and links

1. S. H. Lee, S. L. Lee, and H. Y. Kim, "Electro-optic characteristics and switching principle of a nematic liquid crystal cell controlled by fringe-field switching," Appl. Phys. Lett. **73**(20), 2881 (1998).
2. S. H. Lee and Y. J. Lim, "FFS Technology," in *Handbook of Visual Display Technology* (Springer Berlin Heidelberg, 2015), pp. 1–21.
3. A. Buka and N. Eber, *Flexoelectricity in Liquid Crystals: Theory, Experiments and Applications* (World Scientific, 2012).
4. W. Helfreich, "The Strength of Piezoelectricity in Liquid Crystals," Z. Naturforsch. A **26**(5), 833–835 (1971).
5. R. B. Meyer, "Piezoelectric Effects in Liquid Crystals," Phys. Rev. Lett. **22**(18), 918–921 (1969).
6. H. Chen, F. Peng, M. Hu, and S.-T. Wu, "Flexoelectric effect and human eye perception on the image flickering of a liquid crystal display," Liq. Cryst. **42**(12), 1730–1737 (2015).
7. H. Chen, F. Peng, Z. Luo, D. Xu, S.-T. Wu, M.-C. Li, S.-L. Lee, and W.-C. Tsai, "High performance liquid crystal displays with a low dielectric constant material," Opt. Mater. Express **4**(11), 2262 (2014).
8. H. S. Choi, J. H. Kim, H. G. Ham, Y. J. Lim, J. M. Lee, H. S. Jin, R. Manda, M. S. Kim, D.-K. Yang, and S. H. Lee, "P-131: Studies on Flickering in Low Frequency Driven Fringe-Field Switching (FFS) Liquid Crystal Display," SID Symp. Dig. Tech. Pap. **47**, 1610–1613 (2016).
9. K.-C. Chu, C.-W. Huang, R.-F. Lin, C.-H. Tsai, J.-N. Yeh, S.-Y. Su, C.-J. Ou, S.-C. F. Jiang, and W.-C. Tsai, "24.1: A Method for Analyzing the Eye Strain in Fringe-Field-Switching LCD under Low-Frequency Driving," SID Symp. Dig. Tech. Pap. **45**, 308–311 (2014).
10. R. Hatsumi, S. Fukai, Y. Kubota, A. Yamashita, M. Jikumaru, H. Baba, K. Moriya, D. Kubota, K. Kusunoki, Y. Hirakata, J. Koyama, S. Yamazaki, Y. Chubachi, and C. Fujiwara, "FFS-mode OS-LCD for reducing eye strain," J. Soc. Inf. Disp. **21**(10), 442–450 (2013).
11. I. H. Jeong, I. W. Jang, D. H. Kim, J. S. Han, B. V. Kumar, S. H. Lee, S. H. Ahn, S. H. Cho, and C. Yi, "P.101:

#278724 http://dx.doi.org/10.1364/OE.24.029568
Journal © 2016 Received 18 Oct 2016; revised 1 Dec 2016; accepted 2 Dec 2016; published 13 Dec 2016

Optics EXPRESS

Investigation on Flexoelectric Effect in the Fringe Field Switching Mode," SID Symp. Dig. Tech. Pap. **44**, 1368–1371 (2013).
12. D.-J. Lee, G.-Y. Shim, J.-C. Choi, J.-S. Park, J.-H. Lee, J.-H. Baek, H. C. Choi, Y. M. Ha, A. Ranjkesh, and H.-R. Kim, "Transient flickering behavior in fringe-field switching liquid crystal mode analyzed by positional asymmetric flexoelectric dynamics," Opt. Express **23**(26), 34055–34070 (2015).
13. T. Tsuruma, Y. Goto, A. Higashi, M. Watanabe, H. Yamaguchi, T. Tomooka, and H. Kikkawa, "Novel image sticking model in the fringe field switching mode based on the flexoelectric effect," in *EuroDisplay* (2011), pp. 13–16.
14. D. Xu, F. Peng, H. Chen, J. Yuan, S.-T. Wu, M.-C. Li, S.-L. Lee, and W.-C. Tsai, "Image sticking in liquid crystal displays with lateral electric fields," J. Appl. Phys. **116**(19), 193102 (2014).
15. J.-W. Kim, T.-H. Choi, T.-H. Yoon, E.-J. Choi, and J.-H. Lee, "Elimination of image flicker in fringe-field switching liquid crystal display driven with low frequency electric field," Opt. Express **22**(25), 30586–30591 (2014).
16. S.-W. Oh, J.-H. Park, J.-H. Lee, and T.-H. Yoon, "Elimination of image flicker in a fringe-field switching liquid crystal display by applying a bipolar voltage wave," Opt. Express **23**(18), 24013–24018 (2015).
17. S.-W. Oh, J.-H. Park, J.-M. Baek, T.-H. Choi, and T.-H. Yoon, "Effect of electrode spacing on image flicker in fringe-field-switching liquid crystal display," Liq. Cryst. **43**(7), 972–979 (2016).
18. M. S. Kim, P. J. Bos, D.-W. Kim, D.-K. Yang, J. H. Lee, and S. H. Lee, "Flexoelectric effect in an in-plane switching (IPS) liquid crystal cell for low-power consumption display devices," Sci. Rep. **6**, 35254 (2016).
19. K. S. Ha, C. W. Woo, S. S. Bhattacharyya, H. J. Yun, H. S. Jin, Y.-K. Jang, and S. H. Lee, "Analysis of optical bounce associated with two- step molecular reorientation in the fringe-field switching mode," Liq. Cryst. **39**(1), 39–45 (2012).

1. Introduction

As one of preferred liquid crystal display (LCD) technologies for portable devices, fringe-field switching (FFS) mode is widely used owing to its high-transmittance, high-aperture ratio, wide-viewing angle, and touch-screen tolerance [1,2]. Low-frequency driving is a promising approach to reduce power consumption when displaying static images, which is especially of importance for mobile devices. In this driving method, the pulse duration of the applied signal frames becomes longer than the time the liquid crystal directors physically respond to the field polarity, thereby gaining net electric polarity along the unidirectional electric field vector. This head-tail symmetry breaking of liquid crystals gives rise to flexoelectric effect in terms of a coupling with the elastic distortion [3–5], and such an unusual phenomenon causes a quite obvious spatial difference of optical transmittance between the frames of opposite field-polarities, hence showing the image-flickering even detected by human eyes [6–14]. Therefore, despite of the huge advantage in power consumption, the adoption of the low-frequency driving might not be acceptable until the issue is solved. While it is well known that the combination of quadratic dielectro- and linear flexoelectro-optic effects causes image-flickering in FFS mode and the mechanism of the electromechanical coupling is thoroughly understood, an acceptable solution has not been presented. However, research reports [6,15–17] on this issue have proposed a few methods for reduction of the image-flickering. For instance, 1) controlling the physical properties of liquid crystals, such as dielectric or flexoelectric anisotropy, would reduce the image-flickering. The liquid crystal with negative dielectric anisotropy ($\Delta\varepsilon < 0$) gives rise to less tilt distortion above the electrode and exhibits less deviation of the transmittance between the opposite frames, which results in weaker image-flickering [6]. Also, it has been reported that controlling flexoelectric anisotropy, that is, reducing the difference in the splay (e_s) and bend (e_b) flexoelectric coefficients $\Delta e = e_s - e_b$ would decrease the image-flickering [15]. 2) Another approach is to modify the drive waveform. For example, by applying a bipolar signal voltage adjusted to provide a similar transmittance between the frames [16]. However, the first and the second approaches will require high-cost materials and complication of signal-matrix design due to necessity of two-transistors, respectively. 3) More recently, adjusting electrode-spacing in the FFS cell, also, shows reduction in the image-flickering at the optimized structure [17]; however, the degree of the image-flickering can be controlled within only a limited range.

Optics EXPRESS

Here, while using positive dielectric anisotropy ($\Delta\varepsilon > 0$) materials, we propose more practical solution based on thorough understanding of principle mechanism of the image-flickering in terms of the spatial symmetry of electric field formation in FFS mode. This approach, related to controlling the thickness of the insulation layer between the pixel and common electrodes, is a more fundamental and straightforward way to improve the image-quality. Moreover, our new approach leads to an efficient and intuitive solution to issues regarding the flexoelectric effect, and allows for low-power consumption in a practical display application.

2. Flexoelectric effect in nematic liquid crystals

The flexoelectric effect is a coupling between mechanical deformation and electric polarization in liquid crystals. If the shape of the molecules is not perfectly rod-like, and if there is a molecular dipole moment, the flexoelectric effect can be significant. When the head of molecules is aligned in one direction so the head-tail symmetry is broken, net electric polarity induces a mechanical deformation or vice versa. In this context, the net polarization can be described as,

$$P_f = e_s \boldsymbol{n}(\nabla \cdot \boldsymbol{n}) + e_b \boldsymbol{n} \times (\nabla \times \boldsymbol{n}), \tag{1}$$

where $\boldsymbol{n}$, e_s, and e_b denote unit vector of liquid crystal director, splay and bend flexoelectric coefficients, respectively [2]. The flexoelectric coefficients, which are based on the statistical approach, are expressed as $e_s = \alpha(2\mu_{\square} K_{11}/k_B T)(N \cdot a/b)^{1/3}$ and $e_b = \alpha(\mu_{\perp} K_{33}/2k_B T)(N \cdot b/a)^{2/3}$, where a/b and α are aspect ratio and the angle of molecular anisotropy; μ, k_B, T, and N are dipole moment, Boltzmann constant, temperature, and molecular excess number [3,4]. The system under the dielectric and flexoelectric effects of the liquid crystals can be expressed by elastic free energy density, dielectric and flexoelectric free energies, $f = f_{elas} + f_{dielec} + f_{flexo}$,

$$f_{elas} = \frac{1}{2}\left(K_{11}[\nabla \cdot \boldsymbol{n}]^2 + K_{22}[\boldsymbol{n} \cdot (\nabla \times \boldsymbol{n})]^2 + K_{33}[\boldsymbol{n} \times (\nabla \times \boldsymbol{n})]^2\right), \tag{2}$$

$$f_{dielec} = -\frac{1}{2}\varepsilon_0 \Delta\varepsilon (\boldsymbol{n} \cdot \boldsymbol{E})^2, \tag{3}$$

$$f_{flexo} = -[e_s \boldsymbol{n}(\nabla \cdot \boldsymbol{n}) + e_b \boldsymbol{n} \times (\nabla \times \boldsymbol{n})] \cdot \boldsymbol{E}. \tag{4}$$

3. Results and discussion

We prepared a FFS mode cell as illustrated in Fig. 1. An insulation layer (SiO_2) was sandwiched between transparent indium-tin-oxide layers of interdigitated pixel-electrode with width (space) w (l) = 3 (4) μm (prepared by photo-lithography) and of plane common-electrode on a glass substrate. After a polyimide homogeneous alignment layer was spin-coated on both substrates, a rubbing process was performed with rubbing angle 10° to the long-direction of the interdigitated electrodes. And then, nematic liquid crystal (MLC-6252, Merck) was filled into the cell with the gap d, which is maintained by 4 μm diameter-sized ball spacers. The polarizing optical microscopy (POM) images were captured using a high-speed camera (Phantom v211, Vision Research) and were compared to the numerical simulation images, which were done by a commercialized simulator using the finite element method (TechWiz LCD, Sanayi system) as shown in Fig. 1.

Optics EXPRESS

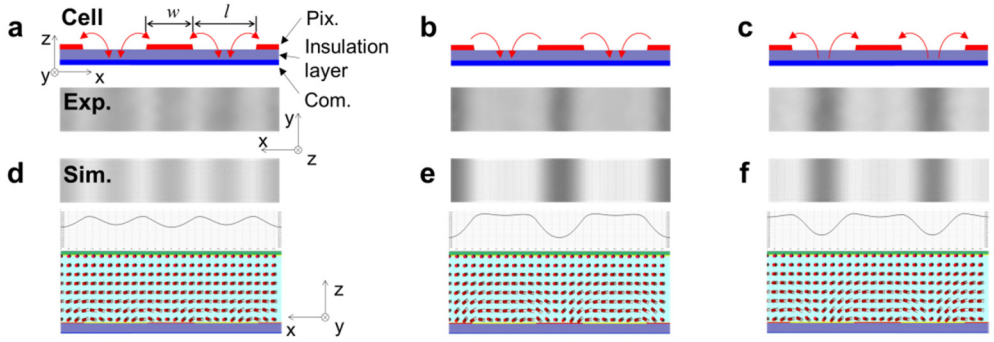

Fig. 1. Flexoelectric effect in a fringe-field switching (FFS) liquid crystal cell. (a-c) Cell schematics and POM images driven at f = (a) 60 Hz and (b, c) 1 Hz at 6.2 V (50% of maximum transmittance) in (b) positive and (c) negative frames. The red arrows represent the direction of electric fields. (d-f) Simulated optical appearance and director fields at (a) e_s (e_b) = 0 (0) and (b, c) e_s (e_b) = 15 (–5) in (b) positive and (c) negative frames at 6.2 V.

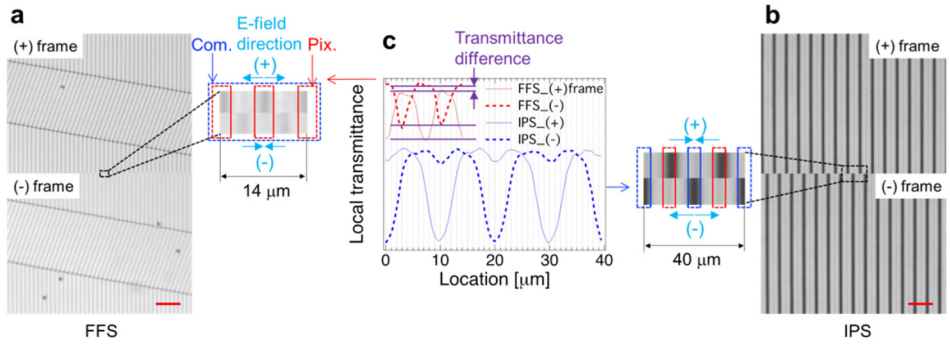

Fig. 2. Experimental investigation of the flexoelectric effect in FFS and IPS modes driven by 1 Hz at 6.2 V. POM images of positive and negative frames in (a) FFS and (b) IPS modes. Scale bars are 40 μm. (c) Local transmittance curves with respect to the location in the insets in (a, b).

The systematic acquisition (under 200 frames per second (fps) with the exposure time < 5 ms) of the POM images in sequential frames was enabled while positive and negative polarities of the applied electric fields with driving frequency f = 60 and 1 Hz. In Fig. 1(a)-1(c), the electric field formation is illustrated for (a) alternating field direction, (b) positive and (c) negative frames. Figure 1(d)-1(f) show the simulated images based on the [2 × 2] extended Jones matrix method with e_s (e_b) = 0 (0) and 15 (–5) pC/m in (d) and (e, f) respectively; the rest of the liquid crystal properties is identical to that used in the experiment.

The details of the flexoelectric effect regarding the optical effect can be thoroughly explored by the director field from the numerical simulation, which is, in this study, highly consistent to the experimental result. Such effects in FFS and in-plane switching (IPS) modes are compared to demonstrate generic reason of the image-flickering. In Fig. 2, the local transmittance curves show different behavior with respect to the location on the electrodes. In IPS, although the local transmittance is spatially shifted upon field polarity, degree of brightness in each frame is similar unlike in FFS as shown in Fig. 2(c) [18]. Assuming the transmittance change is not distinguishable by the spatial resolving power of human eyes, the degree of transmittance in each frame would be the most important factor for the image-flickering based on the human eye perception. Thus, we focus on the symmetry of the electric fields in both FFS and IPS modes, which is caused by the electrode structure in the cells. As schematically described in Fig. 3(a), when the electric field in the (-) frame is inverted by the axis along the light travelling, it is the same to the (+) frame for IPS mode, but not for FFS

Optics EXPRESS

mode. This is also in a good agreement with the comparison between the local transmittances as shown in Fig. 3(b). Note that the brightness of (-) frame is higher than that of (+) frame as also shown in both simulation and experimental results in Fig. 1 - Fig. 3. This is because the electric potential on the area above the space between pixel-electrodes in (-) frame is relatively lower than the potential on the area above electrodes in (+) frame. In (-) frame, the field vector begins from the common-electrode under the insulation layer; on the other hand, in (+) frame, it begins from a pixel-electrode, which is directly in contact with the liquid crystal layer, so that overall director tilt angle is relatively lower in (-) frame than that in (+) frame. Thus, the liquid crystal director between pixel-electrodes is more twisted, resulting in slightly higher transmittance in (-) frame.

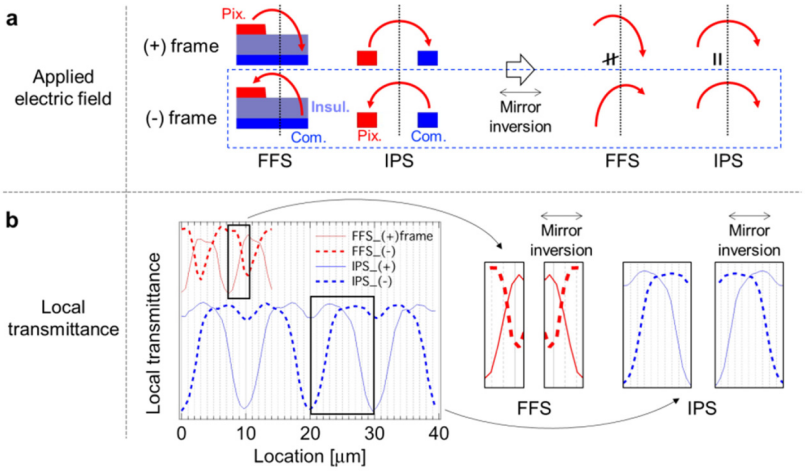

Fig. 3. Symmetry argument of applied electric fields and local transmittance in FFS and IPS modes. (a) Schematic illustration of the field symmetry for positive and negative frames. The mirror inversion of the fields is the same for both frames in IPS but not in FFS mode. (b) Experimental comparison between the local transmittance and its horizontal mirror inversion.

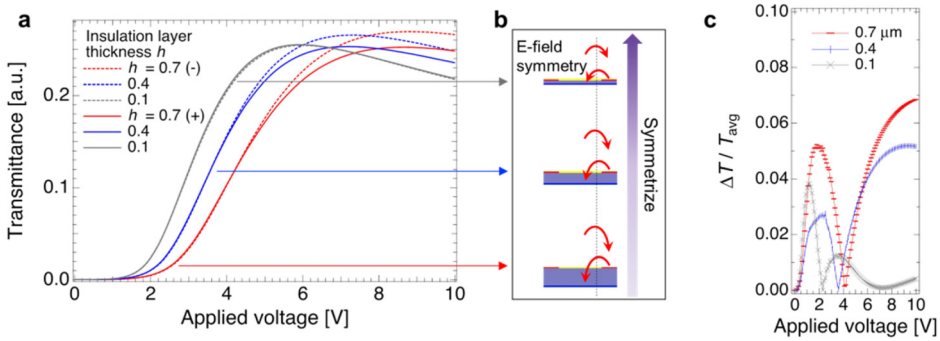

Fig. 4. Effect of the thickness of an insulation layer. (a) Voltage-dependent transmittance without and with flexoelectric effect in positive and negative frames. (b) Schematic description of the field-symmetrization by changing the insulation layer. (c) Voltage-dependent transmittance difference $\Delta T / T_{avg}$ with respect to the thickness of the insulation layer.

This difference in FFS mode should be caused by the electrode structure that the interdigitated pixel- and the plane common-electrode are separated by the thickness of the insulation layer. Therefore, the electric field symmetry should be enhanced by reducing the thickness of the insulation layer as shown in Fig. 4. We run the simulation by varying the insulation layer thickness h = 0.7, 0.4, and 0.1 μm with dielectric constant ε = 3.8. The voltage-dependent transmittance curves for (+) and (-) frames in Fig. 4(a) become

Optics EXPRESS

remarkably identical at h = 0.1 μm. And as schematically shown in Fig. 4(b), one can expect the electric field would be symmetrized as h is reduced. The normalized transmittance difference, $\Delta T / T_{avg} = 2 \times (T_+ - T_-) / (T_+ + T_-)$, where T_+ and T_- are the transmittance at (+) and (-) frames, respectively, also shows the significant reduction of the difference between the frames. Note that $\Delta T / T_{avg}$ below the threshold voltage does not imply crucial meaning for the image-quality because the transmittance difference between frames in Fig. 4(a) is almost negligible to human eyes.

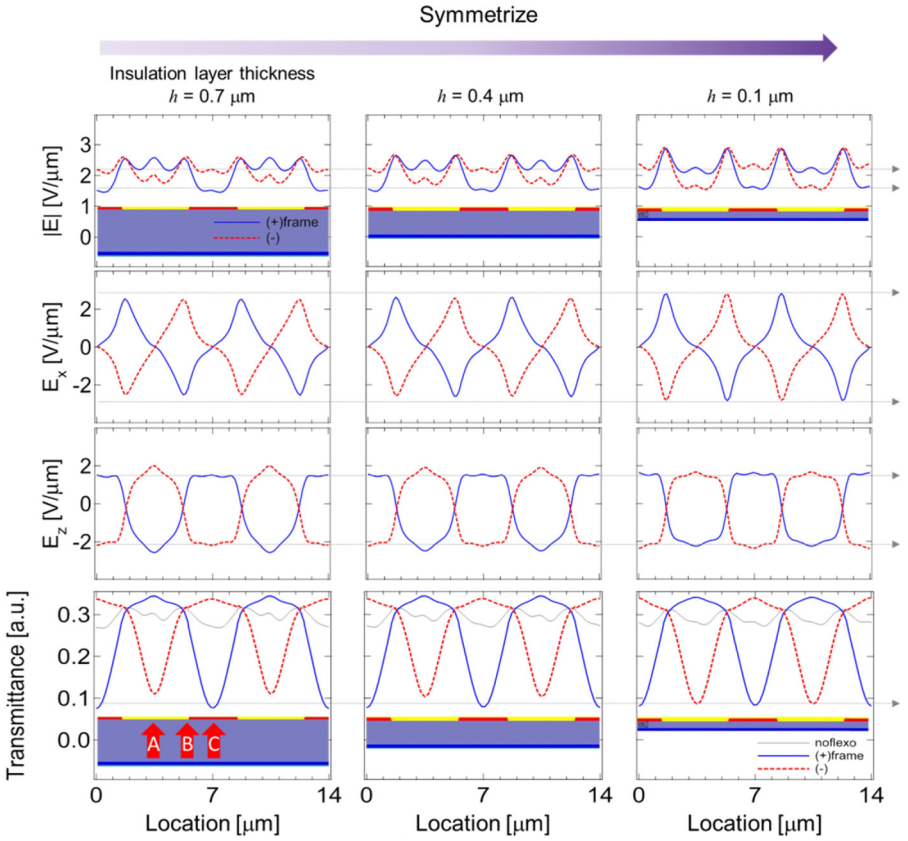

Fig. 5. Symmetrization of the applied electric fields by changing the insulation layer thickness at maximum transmittance. Gray lines indicate the magnitude difference with respect to the h.

Now, we discuss on the electric field components regarding the local transmittance for the symmetry arguments. Here, the symmetry means, again, the electric field formation and the local transmittance between (+) and (-) frames are identical when the field in one of the frames is mirror-inverted. The spatial distribution of electric field strength (at $0 < x < 14$ μm and z = 0.32 μm in the liquid crystal layer) is calculated by Laplace's equation. In the first row in Fig. 5, the magnitude of the electric field along the location x becomes similar for each frame as h becomes reduced. We denote three important locations for further analysis, those are, A: above the space between pixel-electrodes, B: above the edge of the electrodes, and C: above the electrodes as indicated in left-bottom plot in Fig. 5. In details, at A, as shown in the first row in Fig. 5, the magnitude of the electric fields for both frames decrease, while it increases at B as h reduced. By breaking the field vectors into x and z components as plotted in second and third rows in Fig. 5, E_x and E_z can be more closely analyzed. Again, as h is reduced, the highest magnitude of the x-component becomes stronger at B and that of z-component becomes weaker at A. These imply that, because the plane common-electrode gets

Optics EXPRESS

closed to pixel-electrode (the thickness of the insulation layer gets thinner), the field strength becomes stronger at the edge region of electrodes while the field becomes more evenly distributed over the region between pixel electrodes; however, the behavior of the local transmittance curves on these region is somehow unusual and counterintuitive unlike the context considering only dielectric effect. Assuming pure dielectric effect would exist, the local transmittance at A should *increase* by reducing h owing to the suppression of the director tilt (due to the reduced strength of E_z), which would amplify the director twist, and the strengthened x-component at B would make the stronger twist torque that could give rise to the twist at A as well.

However, according to the result in the last row in Fig. 5, the local transmittance *decreases* at A. The reason of this behavior can be analyzed such that, for instance in the (-) frame, the flexoelectric effect at the area near A is *constructive* because the direction of flexoelectric polarization is the same as the electric field direction while the effect at the area near C is *destructive* because the flexoelectric polarization direction is opposite to the electric field direction [18]. Therefore, at A, splay deformation becomes significant although the field strength becomes strong as h gets reduced and it amplifies the director tilt, resulting in the reduced local transmittance. Consequently, the similar degree of the local transmittance at A between (+) and (-) frames takes place and the image-flickering can be significantly reduced because the overall transmittance becomes similar.

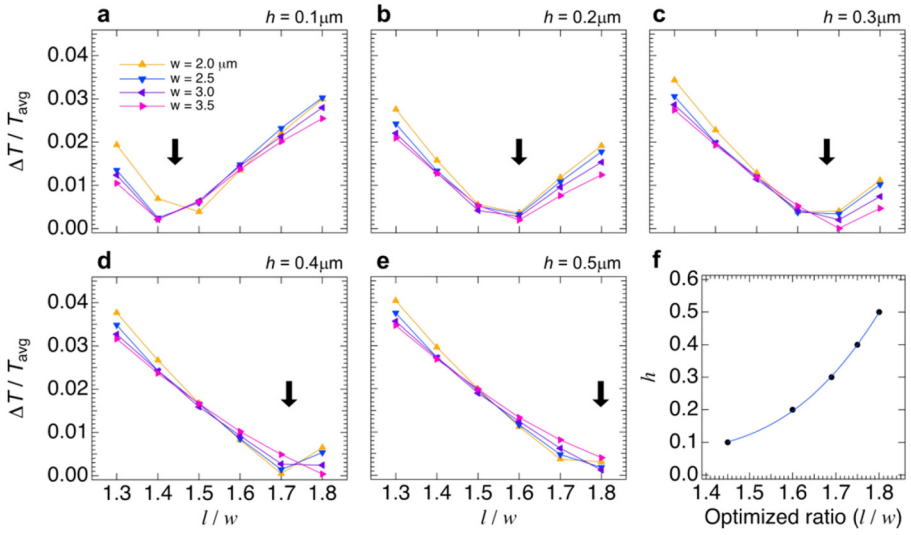

Fig. 6. (a-e) Calculated transmittance difference $\Delta T / T_{avg}$ with respect to the ratio between the space between electrodes to the electrode width (l / w) at various thicknesses of the insulation layer at maximum transmittance. The black arrows indicate the minimum $\Delta T / T_{avg}$. (f) Non-linear relation between the optimized l / w as a function of the h.

Hereafter, we extend the dependent variables on the symmetry of the electric field formation: from the thickness of the insulation layer to an optimized thickness with respect to the ratio of the space (l) between electrodes to the electrode width (w), because we find that the symmetry of the field formation does not uniquely depend on the thickness of the insulation layer. The main reason is that the common-electrode is a plane electrode that is not in the same layer with the patterned pixel-electrodes. Therefore, the x- and z-components of the electric field vector contribute unevenly to the symmetry of the electric field formation, i.e., the electric field vector in the region above the electrodes and above the space between electrodes differently consist of the field components. This is well proved by the transmittance difference as shown in Fig. 6. Depending on h, a relatively optimized l / w (h) exists, that is, ~1.45 (0.1 μm), ~1.60 (0.2 μm), ~1.70 (0.3 μm), ~1.75 (0.4 μm) and ~1.80 (0.5

Optics EXPRESS

μm) as shown in Fig. 6(a)-6(e), respectively. This result clearly demonstrates the dependent variables determining the electric field symmetry are not only h but also l / w, and those are the most fundamental factors to take into account, and it provides a direction to design the electrode structure from an engineering perspective. Additionally, the result is valuable because the optimum h is in the range from 0.1 to 0.5 μm with respect to the range of variation in the l / w from 1.4 to 1.8, which is mostly in common in practical fabrication process. Furthermore, Fig. 6(f) shows that, as the l / w increases, the h becomes larger. Looking back to the electric field formation of FFS mode in Fig. 3(a), it cannot be possible to achieve symmetric electric fields with very thick insulation layer, thereby meaning that the symmetric field formation would not be found if the h is too thick. On the other hand, as the optimized l / w become smaller than 1.45, the h ~0.1 μm is favored.

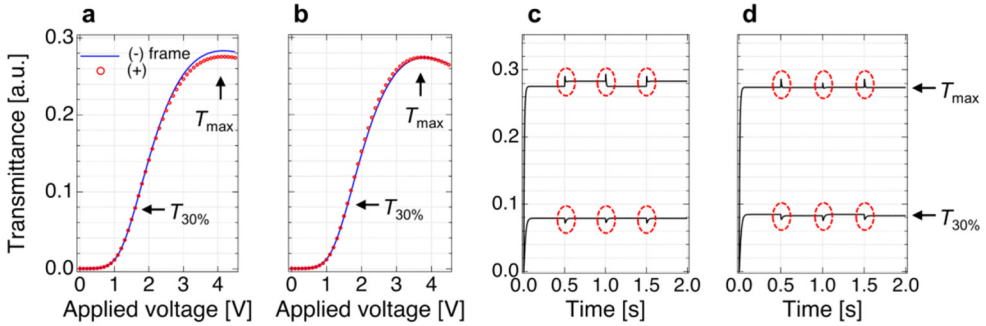

Fig. 7. Comparison of reduced image-flickering for two structural conditions (l / w = 1.3, w = 3.5 μm, h = 0.3 μm for (a,c)) and (l / w = 1.7, w = 3.5 μm, h = 0.3 μm for (b,d)). (a,b) Voltage-dependent and (c,d) time-dependent transmittances when there are (a,c) image-flickering and (b,d) reduced image-flickering. The red circles in (c-d) indicate some known phenomenon during electro-optic switching in FFS mode, so called optical bounce [19].

At last, the voltage-dependent and time-dependent transmittances for two structural conditions have been compared in Fig. 7(a) and 7(b) and Fig. 7(c) and 7(d), respectively. One can clearly notice that the image-flickering becomes almost completely eliminated in an optimized condition. For instance, the image-flickering (at T_{max}) is clearly observed with the structural condition (l / w = 1.3, w = 3.5 μm, h = 0.3 μm) as shown in Fig. 7(a) and 7(c), but almost no transmittance difference between frames with the structural condition (l / w = 1.7, w = 3.5 μm, h = 0.3 μm) as shown in Fig. 7(b) and 7(d). Although the image-flickering in static characteristic becomes significantly reduced, there are still some optical bumps in the field-transient moments as indicated by red-circles in Fig. 7(c) and 7(d), so called optical bounce [21]. This phenomenon is an inherent property of the FFS mode that takes place at the field-off moment. In the field-on state, the directors are twisted on the area above an electrode and are splayed/bent on the area above the edge of an electrode. Upon removal of the field, the splay/bend deformation is released prior to the twist deformation; thereafter, momentarily, extra twist deformation occurs owing to the preceding release of the splay/bend, and the duration of this optical bounce is short. In an applied voltage for $T_{30\%}$ of the transmittance, the behavior of the optical bounce is much reduced as compared with that in T_{max}. Fundamentally, the optical bounce is much less important factor to image flickering than the transmittance difference between frames, and more importantly, this transmittance difference can be almost eliminated in the optimized electrode structure.

4. Conclusion

We have thoroughly investigated the key reason of image-flickering in low-frequency driving fringe-field switching (FFS) mode designed for low-power consumption liquid crystal display devices, and have proposed a practical solution and the engineering view point to design the

Optics EXPRESS

electrode structure to eliminate it. The flexoelectric effect in liquid crystals is a coupling between mechanical deformation and electrical polarization and when low-frequency electric field is applied, the effect becomes significant and appears optically noticeable. We have shown that a key issue related to this effect in FFS devices is that the electric fields in FFS mode are asymmetric upon the positive and negative frames as compared with the IPS mode. Therefore, to reduce the image-flickering, it is fundamentally important to improve the symmetry of the electric field formation. By optimizing the thickness of the insulation layer with respect to the ratio of the space between electrodes to the electrode width, the field formation becomes highly symmetric. As a result, the local transmittance curves and voltage-dependent curves for the positive and negative frames become identical, and results into significant elimination of the image-flickering issue in FFS mode. The results of this work clearly motivate the way of designing practical liquid crystal display devices having low-power consumption via the application of low-frequency driving.

Funding

Basic Research Laboratory Program (2014R1A4A1008140) through the Ministry of Science, ICT & Future Planning; Basic Science Research Program (2016R1D1A1B01007189) through the National Research Foundation of Korea (NRF) funded by Ministry of Education.

Acknowledgments

Prof. D.-K. Yang thanks to the supports from BOE Co.